Claremont Colleges
Scholarship @ Claremont

All HMC Faculty Publications and Research

HMC Faculty Scholarship

Theoretical Studies of Electron Transfer in Metal Dimers: XY+→X+Y, Where X, Y=Be, Mg, Ca, Zn, Cd

Robert J. Cave
Harvey Mudd College

David V. Baxter
California Institute of Technology

William A. Goddard III
California Institute of Technology

John D. Baldeschwieler
California Institute of Technology

Recommended Citation

Theoretical studies of electron transfer in metal dimers: XY⁺ → X⁺Y, where X, Y=Be, Mg, Ca, Zn, Cd

Robert J. Cave,[a] David V. Baxter,[b] William A. Goddard III, and John D. Baldeschwieler

Contribution No. 7525 from the Arthur Amos Noyes Laboratory of Chemical Physics, California Institute of Technology, Pasadena, California 91125

The electronic matrix element responsible for electron exchange in a series of metal dimers was calculated using *ab initio* wave functions. The distance dependence is approximately exponential for a large range of internuclear separations. A localized description, where the two nonorthogonal structures characterizing the electron localized at the left and right sites are each obtained self-consistently, is found to provide the best description of the electron exchange process. We find that Gaussian basis sets are capable of predicting the expected exponential decay of the electronic interactions even at quite large internuclear distances.

I. INTRODUCTION

Electron transfer reactions are important processes throughout biology, chemistry, and physics. Homogeneous[1] and heterogenous[2] redox reactions, biological energy transduction,[3,4] gas phase atom–molecule reactions,[5] and the recently developed Scanning Tunneling Microscope[6] are all systems in which electron tunneling plays an integral role. The ubiquity of electron transfer reactions clearly makes it desirable to gain a fundamental understanding of the factors that influence the rates of these reactions.

Considerable advances have been made in the quantitative assessment of the role of the surrounding medium (outer sphere effects) upon electron transfer.[7-11] While such effects play some role in all of the above processes, the central feature in controlling the electron transfer rate at large inter-reactant separations is the degree of electronic interaction between the donor and acceptor.[8-12] These interactions have been discussed qualitatively but quantitative assessments of the variation of the electronic interaction from system to system, as well as its distance and orientation dependence, have been limited.

Several studies have examined the decrease in the rate of electron transfer with distance between two fixed centers in glassy matrices.[13-15] This decrease is primarily controlled by the decay with distance of the electronic interaction, for which functional forms were assumed. The role of the intervening medium between pairs of redox centers on the decay of the electron transfer rate has been investigated by Beratan and Hopfield[16] and by Larsson,[17,18] using extended Hückel-type wave functions to estimate the electronic interactions. *Ab initio* electronic structure techniques have been applied to the study of the Fe(H₂O)₆³⁺/²⁺ and Ru(NH₃)₆³⁺/²⁺ self-exchange reactions by Newton and co-workers.[19-21] Dis-

tance and surface-corrugation effects on the tunneling current in the scanning tunneling microscope have been examined using square-well-type wave functions, as well as more detailed models.[21-24]

In this article we address some of the questions regarding the electronic interaction using results from *ab initio* electronic structure calculations for diatomic systems. In particular, we examine the energy dependence of the electronic interaction and its dependence on the atoms and orbitals involved in the transfer. Also, we address the sensitivity of the interaction to the method of calculation. In Sec. II, the quantity characterizing the electronic interaction, T_{BA}, is introduced and discussed for a one-electron model. In Sec. III, T_{BA} as a function of distance is compared for a variety of symmetric, diatomic charge transfer systems. In Sec. IV, several methods of calculating T_{BA} are compared, and in Sec. V, charge transfer interactions are compared for heteronuclear diatomic systems. Our conclusions are presented in Sec. VI.

II. T_{BA} AND ONE-ELECTRON SYSTEMS

In order to outline the procedures used, consider starting with the system A in which, for example, a neutral Cd is on the left (center A, with wave function Φ_{Cd}^L) and an ionized Cd is on the right (center B, with wave function $\Phi_{Cd^+}^R$). The total wave function for A is thus

$$\Phi_A = \hat{A} \left[\Phi_{Cd}^L \Phi_{Cd^+}^R \right], \qquad (1)$$

where $\hat{A}$ indicates that the total wave function for Cd *and* Cd⁺ is antisymmetric (to satisfy the Pauli Principle). After electron transfer, we have system B with an ionized Cd on the left (wave function $\Phi_{Cd^+}^L$) and a neutral wave function on the right (wave function Φ_{Cd}^R). Thus the total wave function for B is

$$\Phi_B = \hat{A} \left[\Phi_{Cd^+}^L \Phi_{Cd}^R \right]. \qquad (2)$$

Since the valence electronic wave function of Cd is $(5s)^2$ and that of Cd⁺ is $(5s)^1$, we can think of this electron transfer in terms of removing an electron from the left $5s$ orbital and placing it in the right $5s$ orbital. However, this charge transfer also changes the shielding of the various orbitals and, as a

result, the shapes of the $5s$ orbital and of the core orbitals change upon charge transfer. Indeed, these shape readjustment effects are sufficiently important that the optimum Hartree–Fock (HF) wave functions have the localized form of Eqs. (1) or (2) rather than the usual delocalized form in terms of symmetry functions (σ_g, σ_u, etc.).

Starting out at $t = 0$ with the system in $|A\rangle$, the probability, $P_{BA}(t)$, of finding the system in $|B\rangle$ at time t, if A and B are the same atomic species (and neglecting all other electronic states of A and B), may be written as

$$P_{BA}(t) = \sin^2\left[\frac{T_{BA}t}{\hbar}\right].$$ (3)

The quantity T_{BA} in Eq. (3) is defined as

$$T_{BA} = \frac{H_{BA} - S_{AB}H_{AA}}{1 - |S_{AB}|^2},$$ (4)

where

$$H_{BA} = \langle B|\hat{H}|A\rangle,$$ (5a)

$$H_{AA} = \langle A|\hat{H}|A\rangle,$$ (5b)

$$S_{AB} = \langle A|B\rangle,$$ (5c)

and $\hat{H}$ is the full Hamiltonian of the system. The quantity T_{BA} is responsible for the rate of oscillation between states $|A\rangle$ and $|B\rangle$, and thus controls the rate of charge exchange in such systems. It is T_{BA} that will be evaluated as a measure of the strength of the charge exchange interactions for the various diatomic systems in the present article.

In extended systems, where a single reactant electronic state decays into a continuum of product electronic levels, T_{BA} enters the golden rule (GR) rate expression for charge transfer,[8,9,11] as shown in Eq. (6)

$$k_{GR} = \frac{2\pi}{\hbar}|T_{BA}|^2\rho.$$ (6)

In Eq. (6), the Condon approximation[8,9] has been made and ρ then assumes the form of a weighted density of electronic or nuclear states, depending on the system of interest.[1,11] Therefore, in both diatomic and many-atomic systems, T_{BA}, as defined in Eqs. (4) and (5), is intimately related to the frequency of electron transfer.

The simplest symmetric charge exchange system is H_2^+, for which an analytic expression for T_{BA} can be obtained. In this case, $|A\rangle$ is taken as representing an electron in a hydrogenic orbital localized on center A and $|B\rangle$ is defined analogously. T_{BA} then becomes[25]

$$T_{BA} = \frac{Z\alpha \exp(-\alpha R)\left[\frac{2\alpha R}{3} - \frac{1}{\alpha R}\right] + Z\alpha \exp(-3\alpha R)\left[2 + \frac{1}{\alpha R} + \frac{4\alpha R}{3} + \frac{\alpha^2 R^2}{3}\right]}{1 - |S_{AB}|^2},$$ (7a)

$$S_{AB} = \exp(-\alpha R)\left(1 + \alpha R + \frac{\alpha^2 R^2}{3}\right),$$ (7b)

where Z is the effective nuclear charge ($Z = 1$ for H_2^+ at large R), $\alpha = (2mE/\hbar^2)^{1/2}$ ($\alpha = 1$ for H_2^+) in atomic units, and R is the internuclear separation. For R beyond a few angstroms, the first term dominates, the denominator is nearly 1, and one obtains

$$T_{BA} \cong \frac{2Z\alpha^2 R \exp(-\alpha R)}{3}.$$ (8)

This expression therefore provides a means of testing our calculations for H_2^+.

In our calculations of T_{BA} for H_2^+ using *ab initio* electronic structure techniques, standard Gaussian basis sets centered on each atom were used (see the Appendix), augmented by diffuse s functions. The electronic states $|A\rangle$ and $|B\rangle$ were taken to be the ground state variational solutions of the Schrödinger equation at sites A and B in the absence of the second center. T_{BA} was evaluated using these wave functions, as prescribed by Eqs. (4) and (5). The results are shown in Fig. 1. It is seen that from 5 to 9 Å, the *ab initio* results are in excellent agreement with the analytic, exact results. At larger distances, the *ab initio* results begin to diverge and become larger than the exact results. In general, in order for Gaussian functions to describe the exponential decay, it is necessary to have a collection of sufficiently diffuse functions (see Appendix) so that they can combine to yield the expected exponential character.

These results suggest that *ab initio* wave functions can be used to obtain estimates of the size of T_{BA} and its decay as
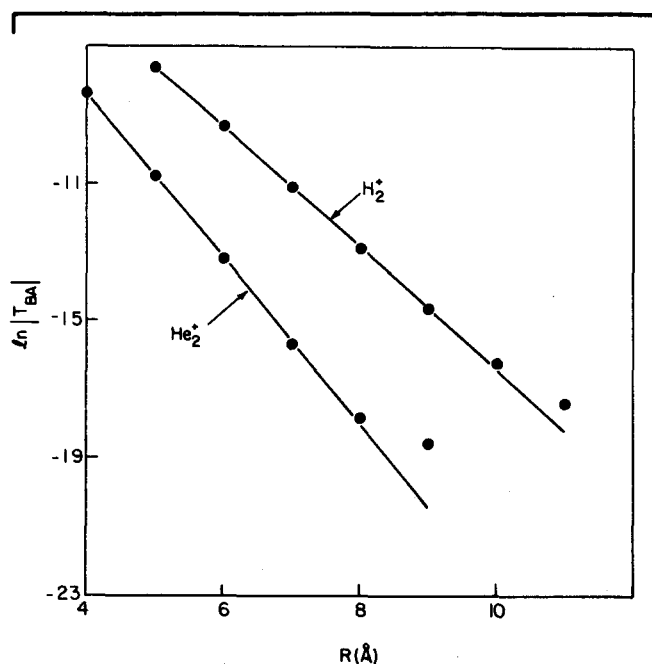

FIG. 1. $\ln|T_{BA}|$ (T_{BA} in hartree) vs R for H_2^+ and He_2^+. For the H_2^+ results, the circles are the results of the present frozen orbital calculations, the solid curve is the natural logarithm of Eq. (7), and the dashed curve (not seen since it is superimposable on the solid line) is the natural logarithm of Eq. (8), the large R form of Eq. (7). For the He_2^+ results, the circles are the results of the present SCF calculations, and the solid curve is a plot of the natural logarithm of the function $T_{BA} = A_1R\exp(-\alpha_1R)$, where $\alpha_1 = (-2mE^{\text{Koopmans}}/\hbar^2)^{1/2}$. E^{Koopmans} is the Koopmans estimate of the He IP, and A_1 is obtained by equating the functional and calculated values of T_{BA} at $R = 5$ Å.

a function of distance. In the next section, we examine the behavior of T_{BA} for many-electron systems.

III. s-ORBITAL TRANSFERS IN THREE-ELECTRON SYSTEMS

In this section, we examine s orbital to s orbital electron transfers in the symmetric charge transfer systems $He_2^+, Be_2^+, Mg_2^+, Zn_2^+, Ca_2^+$, and Cd_2^+. In each case, the atom and ion have the electronic occupations [core] ns^2 and [core] ns^1, respectively. Since there is minimal electronic reorganization of the core upon oxidation or reduction, we refer to these as three-electron systems. For Be_2^+ the $1s$ core electrons are explicitly included in the calculation, and for Zn_2^+ and Cd_2^+, the $3d^{10}$ and $4d^{10}$ cores are included (see the Appendix), but deeper core levels were replaced by effective potentials.[26,27] We found that T_{BA} is insensitive to core readjustments in these cases. Because of the presence of additional electrons, we calculated T_{BA} using a procedure different from that used for H_2^+. For these three-electron systems at finite internuclear separation, the HF wave functions lead to localized AA^+ or A^+A configurations (rather than symmetry orbitals) because the core electrons relax and thus stabilize the localized charge. Thus, we have used these localized HF wave functions (labeled SCF, below) for the three-electron systems in the results of this section (rather than the analogous frozen orbital results as in Sec. II for H_2^+). The consequences of freezing the orbitals for the three-electron systems will be discussed in Sec. IV. As for H_2^+, standard basis sets were augmented by the addition of diffuse functions (s and p sets; see Appendix). Since the left and right localized wave functions are in general composed of nonorthogonal orbitals, T_{BA} was evaluated using the biorthogonalization procedure of Voter and Goddard[28] (see the Appendix).

A. HeHe$^+$

Results for the calculation of T_{BA} for He_2^+ are shown in Fig. 1. The solid line, shown together with the calculated data points, is a plot of

$$T_{BA} = AR \exp(- \alpha^{Koopmans}R), \tag{9a}$$

where

$$\alpha^{Koopmans} = \left[\frac{- 2mE^{He}}{\hbar^2} \right]^{1/2}, \tag{9b}$$

with E^{He} being the Koopmans orbital ionization potential (IP) for He, and A is obtained from equating the function to the calculated T_{BA} at $R = 5Å$. The agreement is quite good from 4 to 7 Å, with deviations appearing beyond 7 Å. From the HF wave function we obtain $\alpha^{Koopmans} = 1.36$ bohr^{-1}, while a least-squares fit of the T_{BA} data from 4 to 7 Å yields $\alpha^{Fit} = 1.38$ bohr^{-1}, in excellent agreement. It is reasonable to expect that T_{BA} for He_2^+ should have a functional form similar to that for H_2^+, since the transfers occur between $1s$ orbitals in both cases (although He_2^+ has some electronic reorganization). At large R, deviations from exponential decay most likely result from deficiencies in the Gaussian basis set. He_2^+ is quite a severe test, however, since the wave functions decay so rapidly. Of the systems discussed here, He_2^+

has the shortest R for which this deviation occurs. For all others, exponential decay is exhibited beyond 11 Å separation, as shown below.

B. Other three-electron systems

Results are shown in Fig. 2 for Be_2^+ over the range of 5 to 13 Å. Least-squares fits to the data points using the functional forms $T_{BA} = A_0\exp(- \alpha_0R), A_1R \exp(- \alpha_1R)$, and $A_2R^2 \exp(- \alpha_2R)$ were performed; the results of the $A_2R^2 \exp(- \alpha_2R)$ fit are shown in the figure. The values of α_0, α_1, and α_2 from these fits are, respectively, 0.663, 0.726, and 0.788 bohr^{-1}; $\alpha^{Koopmans} = (2mE^{Be}/\hbar^2)^{1/2} = 0.786$ bohr^{-1}, in excellent agreement with that from the functional form $T_{BA} = A_2R^2 \exp(- \alpha_2R)$. The quality of the fits was good for all three forms, the first being slightly better than the rest.[29] However, from a comparison of the values of α^{Fit} and $\alpha^{Koopmans}$, it is clear by analogy with the He_2^+ and H_2^+ results that the third form yields the best agreement with the expected large R decay rate of T_{BA}. That is, the third form yields the closest agreement with the exponential decay constant estimated from the Koopmans IP, as was obtained for H_2^+ and He_2^+. (Agreement will vary somewhat with basis set; see Sec. IV D.) It is of interest to explore what causes the form of T_{BA} to change in progressing from He to Be, both of which are ostensibly three-electron systems undergoing s-orbital-to-s-orbital electron transfers. Qualitatively, the cause of this change can be seen by examining the form of the hydrogenic orbitals involved in the transfers. For He, the $1s$ orbital has the form

$$\phi_{1s}^{He} = \frac{\alpha^{3/4}}{\pi^{1/2}} \exp(- \alpha^{He}R), \tag{10}$$

while a hydrogen-like $2s$ orbital (qualitatively similar to the Be $2s$ orbital) has the form
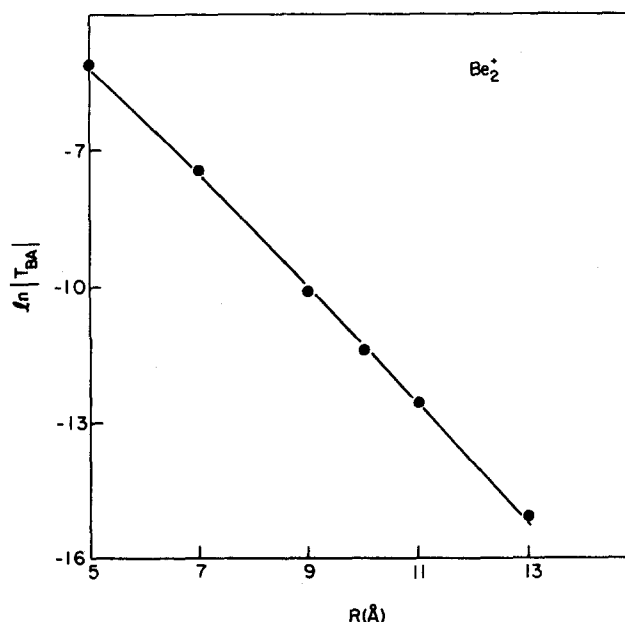

FIG. 2. $\ln|T_{BA}|$ vs R for Be_2^+. The circles are the results of the present SCF calculations. The solid line is a least-squares fit of the functional form $T_{BA} = A_2R^2 \exp(- \alpha_2R)$ to the data. The parameters of the fit are given in Table I.

$$\phi_{2s}^{Be} = \frac{(\alpha^{Be})^{3/2}}{4(2\pi)^{1/2}} (2 - \alpha^{Be}R)\exp(-\alpha^{Be}R). \qquad (11)$$

We have obtained an estimate of a one-electron T_{BA} for Be_2^+ by using the above ϕ_{2s}^{Be} and calculating

$$T_{BA}^{one} = \frac{1}{(1 - S_{lr}^2)} (\langle \phi_{2s}^r | V_r | \phi_{2s}^l \rangle - S_{lr} \langle \phi_{2s}^l | V_r | \phi_{2s}^l \rangle),$$

$$(12)$$

with $V_r = (-Z_{eff}/R_r)$, exactly analogous to the case of T_{BA} for H_2^+. (Note: this is equivalent to assuming that the untransferred charge density is fixed on each center and creates an equivalent effective potential V_r, for which ϕ_{2s}^r is a one-electron eigenfunction.) The first term in parentheses is again dominant, and for $S_{lr} \ll 1$, T_{BA}^{one} becomes[30]

$$T_{BA}^{one} \simeq Z_{eff} \left[\tfrac{1}{2}(1 + \alpha R) - \tfrac{1}{3}\alpha^2 R^2 + \tfrac{1}{6}\alpha^3 R^3 \right]$$

$$\times \exp(-\alpha R). \qquad (13)$$

Thus, the factor multiplying the $\exp(-\alpha R)$ term in T_{BA} is expected to have a polynomial form, which is dependent on the orbitals involved in the electron transfer. Since the hydrogenic Be 2s orbital is a poor approximation to the HF Be 2s orbital, the exact form of T_{BA}^{one} for Be_2^+ is expected to differ from Eq. (13). However, it is just as R becomes large that the transferring electron experiences a hydrogenic potential, and therefore the qualitative aspects of this argument should hold.

For the systems Zn_2^+, Cd_2^+, Mg_2^+ and Ca_2^+, plots of $\ln|T_{BA}|$ are shown in Figs. 3 and 4 (see the Appendix for a description of the quantities plotted in each case). Together with the results of the calculations, the results of fitting these points to the functional form $T_{BA} = A_2 R^2 \exp(-\alpha_2 R)$ are presented. In general, the fit is shown to be quite good, and in
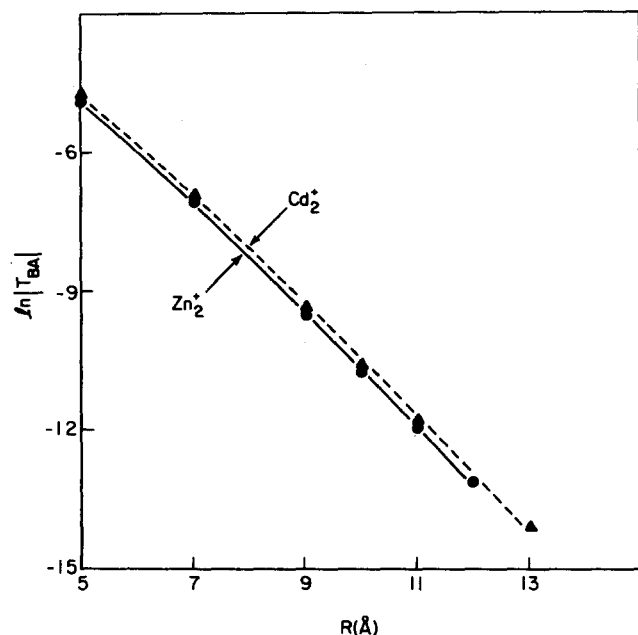

FIG. 4. $\ln|T_{BA}|$ vs R for Mg_2^+ and Ca_2^+. The circles (triangles) are the present Mg_2^+ (Ca_2^+) SCF results, the solid curve (dashed curve) is the least-squares fit to the functional form $T_{BA} = A_2 R^2 \exp(-\alpha_2 R)$ for Mg_2^+ (Ca_2^+). The parameters of the fits are given in Table I.
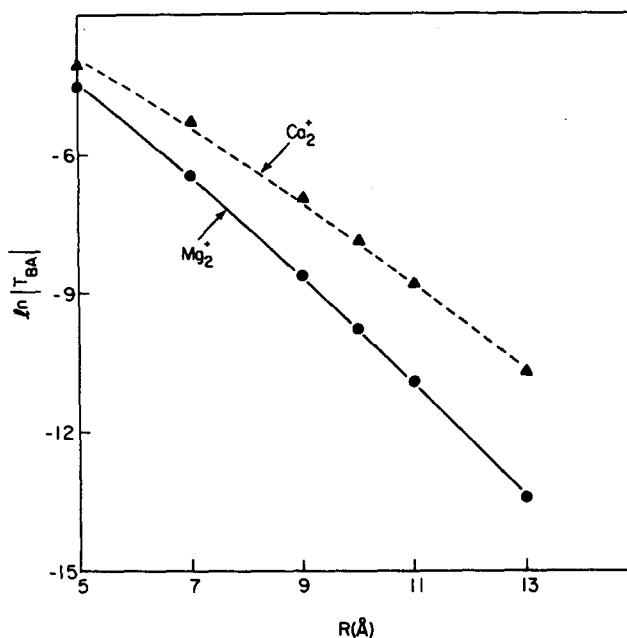
all cases the region over which the decay is approximately exponential is at least from 6 to 12 Å. The parameters of the fits for A_2 and α^{Fit} are given in Table I, together with estimates of α based on Koopmans' IP for the atom ($\alpha^{Koopmans}$), and estimates for α based on the actual IP's for the atoms (α^{IP}). In all cases but Ca_2^+, the agreement between α^{Fit} and $\alpha^{Koopmans}$ is excellent. The Ca_2^+ results appear to be better fit by the functional form $T_{BA} = A_1 R \exp(-\alpha_1 R)$. This may be an artifact of incomplete localization in the initial and final wave functions, thus artificially increasing T_{BA}. Nevertheless, in general, the agreement is very good. The significant difference between $\alpha^{Koopmans}$ and α^{IP} is caused by inaccuracies in the IP's for the present wave functions. Here the quantity of interest to discussions of T_{BA} is $\alpha^{Koopmans}$, since it corresponds to the energies of the wave functions actually used.

The results of Figs. 3 and 4 indicate that atomic size as well as orbital energy can play a role in determining the size of T_{BA}. This is especially apparent when values of T_{BA} are

FIG. 3. $\ln|T_{BA}|$ vs R for Zn_2^+ and Cd_2^+. The circles (triangles) are the present Zn_2^+ (Cd_2^+) SCF results, the solid curve (dashed curve) is the least-squares fit to the functional form $T_{BA} = A_2 R^2 \exp(-\alpha_2 R)$ for Zn_2^+ (Cd_2^+). The parameters of the fits are given in Table I.

TABLE I. Decay constants for symmetric systems.[a]

System	A^{Fit}[b]	α^{Fit}[b]	$\alpha^{Koopmans}$[c]	α^{IP}[d]
Be_2^+	0.108	0.788	0.786	0.828
Zn_2^+	0.106	0.757	0.759	0.831
Cd_2^+	0.111	0.746	0.750	0.813
Ca_2^+	0.086	0.566	0.521	0.670
Mg_2^+	0.108	0.714	0.714	0.750

[a] All quantities in a. u.
[b] From fitting $T_{BA} = A_2 R^2 \exp(-\alpha_2 R)$.
[c] From the Hartree–Fock calculation.
[d] IP from experiment.

compared at a given R for the systems Be_2^+, Zn_2^+, and Cd_2^+, all of which have comparable values of α^{Koopmans}. In this series, T_{BA} increases monotonically with increasing atomic radius. Comparisons with Mg_2^+ and Ca_2^+ are less transparent since α^{Koopmans} is significantly different in these systems compared with the previous three. Of course, atomic size is not the only factor determining the size of T_{BA}, since the overlaps of the core orbitals at each center will differ from system to system. Qualitatively, these overlap terms can be seen to enter T_{BA} as multiplicative factors that are constant as functions of R. However, the present results indicate that the difference in atomic radii can provide a useful qualitative measure of the size of T_{BA}. That is, all other factors being approximately equal, T_{BA} will be largest at a given internuclear separation for transfers between the atoms having the largest atomic radii. Thus, a given value of T_{BA} cannot be simply related to an interatomic distance.

IV. COMPARISON OF METHODS OF OBTAINING T_{BA}

Using Be_2^+ as a model system, calculations of T_{BA} were performed with a variety of types of wave functions and the results were compared with the Be_2^+ SCF results of Sec. III. We discuss these results here.

A. Frozen orbitals

For this case, the composite Be_2^+ wave function was composed of atomic orbitals for Be and Be^+ obtained from HF calculations on the isolated atom and ion, respectively. The orbitals were orthogonalized at each R but were otherwise unchanged from their shapes at infinite separation. The results of calculations of T_{BA} using these frozen atom + ion wave functions are shown in Fig. 5 and are compared with a fit of the SCF results of Fig. 2. From 5 to 9 Å, the shapes of
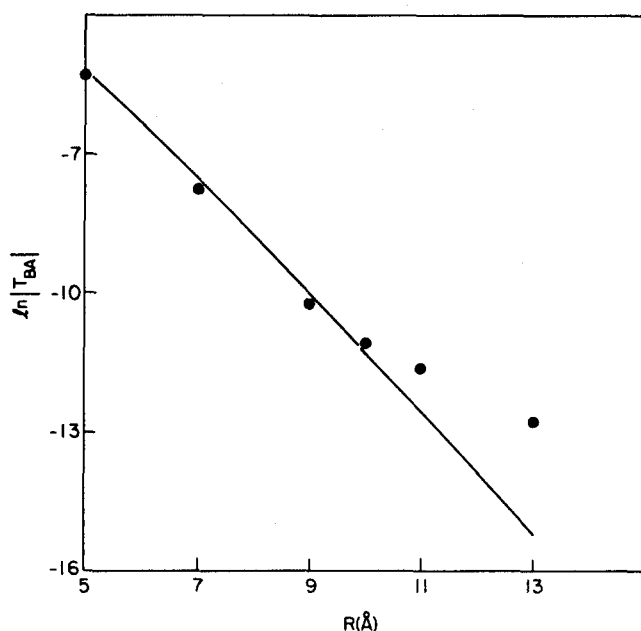
FIG. 5. Comparison of $\ln|T_{BA}|$ vs R for Be_2^+ using SCF and frozen (atom + ion) (see text) wave functions. (The three diffuse-function basis set was used for Be.) The solid curve is from the $A_2R^2 \exp(-\alpha_2 R)$ fit to the SCF results, the circles are the frozen wave function results.
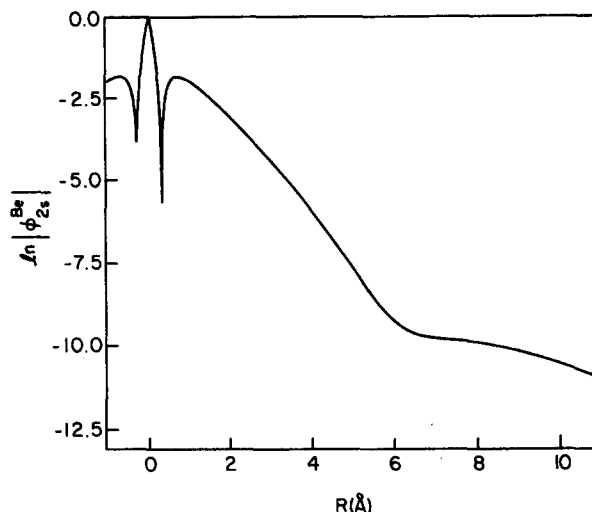
FIG. 6. $\ln|\phi_{2s}^{Be}|$ as a function of R (Å), the distance from the nucleus at which ϕ_{2s}^{Be} is centered. ϕ_{2s}^{Be} was obtained from a Hartree–Fock calculation on Be using the three diffuse-function basis set.

$\ln|T_{BA}|$ vs R for the frozen and SCF results are in excellent agreement, the value of T_{BA} being somewhat larger for the SCF results. Beyond 9 Å, the rate of decay of the frozen orbital results changes abruptly and the agreement becomes poor. We believe this dramatic change indicates that the frozen orbital results are inaccurate at large distances, for reasons similar to the H_2^+ results, since we know of no physical reasons to expect an abrupt change in the decay of T_{BA} with distance at large R. In Fig. 6, a plot of $\ln|\phi_{2s}^{Be}|$ is shown as a function of radial distance. At approximately 6 Å, the rate of decay changes dramatically. Beyond this point, only a single basis function is of appreciable size; thus the wave function decay with R is poorly represented. The good agreement at short R between the SCF and frozen orbital results indicates that the SCF procedure introduces no significant change in the left and right localized wave functions, relative to the pure atom and ion, thus supporting the assertion that the electronic interaction between the centers is weak over this range of R. The observed small size difference between T_{BA} calculated using the frozen and SCF wave functions at short R is most likely due to a slight polarization of the Be 2s orbital due to the presence of the nearby ion, thus increasing T_{BA}. The larger range over which the SCF results are able to obtain a nearly linear decay of $\ln|T_{BA}|$ with distance apparently stems from the incorporation of functions on the second center into the orbitals localized on the first. Since incorporation of the second center functions may partly correct for deficiencies in the very large R portion of the atomic basis sets, this may be partially a basis set superposition effect. However, it would be wrong to immediately assume that T_{BA} is incorrectly calculated as a result of this superposition effect. In fact, the similarity of the slopes at medium and long R suggests that the expected exponentially decreasing interaction between the two centers is being modeled correctly, even with the deficiencies in the large R part of the atomic basis. Calculations using extended diffuse basis sets for each atom would test the origins for the increased range of the SCF calculation's apparent success in computing T_{BA}. Similar results were obtained for other three-electron systems.

B. Frozen orbitals—atom + atom wave functions

These frozen wave functions are similar to the ones used in Sec. IV A, except orbitals appropriate to the neutral species were used to describe both the atom and the ion. The results are presented in Fig. 7 and are seen to be in reasonable agreement with the SCF results from 5 to 9 Å. Similar comments to those of the preceding section apply to the change in decay at large R. Use of this wave function eliminates any electronic reorganization at a center upon loss or gain of an electron. It is thus the many-electron analog of the one-electron calculation of T_{BA} between two fixed potentials. It can be seen that restriction to atomic wave functions (rather than atom + ion wave functions) does not radically alter the size or behavior of T_{BA} over the range of distances where basis set effects are minimal.

A comparison of the frozen wave function results of this section with those of Sec. IV A (and/or the SCF results) indicates that electronic reorganization effects are not of primary importance in determining the size of T_{BA} for Be_2^+. *A priori*, it is not obvious whether changes in the "untransferred" charge distribution will significantly alter the size of T_{BA}. The fact that the frozen atom + atom results are nearly equal to the frozen atom + ion results shows that in this case electronic relaxation has a minor effect on T_{BA}. (In fact, the frozen atom + ion results are slightly *larger* than the atom + atom results at all R.) While this result must certainly be checked for other systems, we would argue that electronic reorganization effects on T_{BA} due to charge readjustments, if important at all, should be most important in small systems such as these light diatom systems. That is, in these light diatomic systems, the "transferring" electron and the untransferred charge density are both localized on single centers and are strongly interacting; thus, one might expect large valence orbital shape changes upon electron transfer.
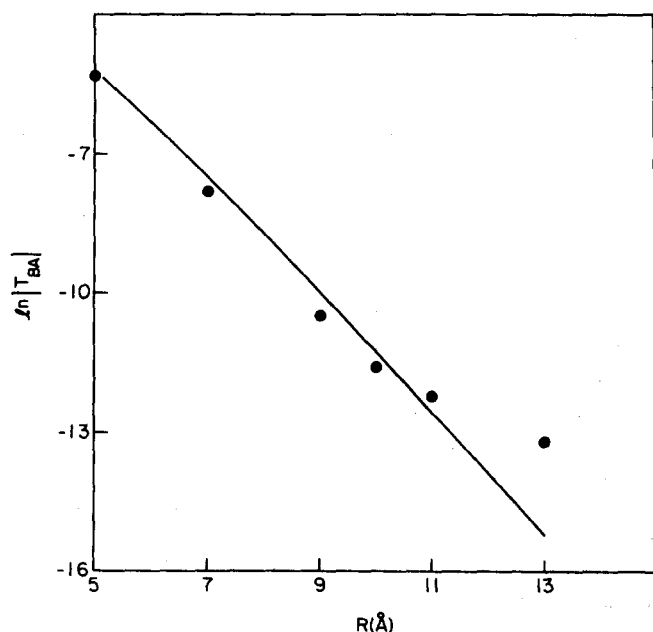
The fact that charge readjustment effects on T_{BA} do not appear to be important here suggests that their effects may be small for larger systems such as, for example, metal atom clusters or large aromatic molecules.

C. Symmetry-restricted systems

In a one-electron symmetric system, T_{BA} is equal to half the energy splitting between the ground state (symmetric) LCAO wave function and the first excited state (antisymmetric) LCAO wave function. In the three-electron case, the T_{BA}'s calcuated using localized and symmetry-restricted wave functions need not be equal and, in general, will not be unless there is minimal electronic reorganization for both the core and valence electrons upon electron transfer. In Fig. 8 we present two types of symmetry-restricted calculations of T_{BA} using a two-diffuse function basis for Be (see Sec. IV D and the Appendix). In one case, the wave functions are obtained self-consistently, with the restriction that they be either symmetric or antisymmetric under inversion. In the second case, the MO's were obtained from symmetric and antisymmetric combinations of Be atomic orbitals, properly orthogonalized at each R, but otherwise unchanged from their infinite R forms. Note, for the three-electron system, the ground state is antisymmetric and the first excited state is symmetric with respect to inversion through the bond midpoint.

Results of the antisymmetric–symmetric wave function estimates of T_{BA} are shown in Fig. 8. As with the results of the preceding two sections, it is seen that the decay of T_{BA} agrees with the SCF results from 5 to 7 Å, after which the symmetry-restricted results diverge from the SCF results, both for the frozen *and* self-consistenly obtained symmetry-restricted results.
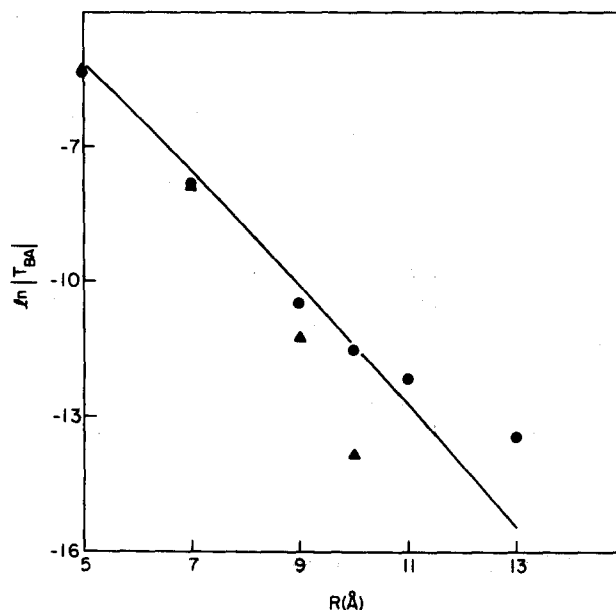

FIG. 7. Comparison of $\ln|T_{BA}|$ vs R for Be_2^+ using SCF and frozen atom + atom wave functions. (The three diffuse function basis set was used for Be.) The labeling is as in Fig. 5.

FIG. 8. Comparison of $\ln|T_{BA}|$ vs R for Be_2^+ using SCF and symmetry-restricted wave functions. (The two diffuse-function basis set was used for Be; see Sec. IV D and the Appendix.) The circles are the frozen orbital symmetry-restricted results, the triangles the self-consistent symmetry-restricted results, and the solid curve is from the $A_2 R^2 \exp(-\alpha_2 R)$ least-squares fit to the SCF results.

It should be noted that for all R examined here, the SCF localized wave function yields a significantly lower energy than the self-consistent symmetry-restricted result, indicating that core relaxation upon localization is energetically more favorable than the energy return from delocalization(i.e., bonding). This should not be surprising for the large R's considered here. As to which description of T_{BA} is to be preferred for this range of R's (and all larger R), two lines of argument suggest that the localized description is the more appropriate. First, the localized results yield a more nearly exponential decay with distance over the range of R considered. Since we assume that exponential decay of T_{BA} at large R is correct, this would suggest the localized results as the more accurate. The symmetry-restricted results show a rather abrupt change in the decay of T_{BA} at larger R (most likely numerical errors in calculating the energy differences), and we know of no reason to assume T_{BA} should behave in this manner. Second, the localized description is a better representation of the actual atomic charge distributions whenever the time scale for electron transfer is long compared with the time for electronic relaxation. This second problem clearly mandates a localized description for long-range electron transfer processes.

D. Basis set sensitivity

SCF calculations were performed for Be_2^+ using three different basis sets: (1) VDZ (see the Appendix) with no diffuse functions, (2) VDZ + two sets of s and p diffuse functions (used in Sec. IV C), and (3) VDZ + three sets of s and p diffuse functions (used in Secs. III and IV A–B). The purpose of these calculations was to test the sensitivity of the calculated value of T_{BA} to the choice of basis. The results are shown in Figs. 9(a) and 9(b) where results from basis sets 1 and 3 and from 2 and 3 are compared, respectively. In Fig. 9(a), it is seen that the results agree at short distances but basis set 1 yields a much more rapidly decaying T_{BA} at larger distances, indicating the importance of diffuse functions. In Fig. 9(b), the results for basis set 2 are shown to be in excellent agreement with those of basis set 3 to 12 Å. The values of A_2^{Fit} and α_2^{Fit} for the two diffuse function basis are 0.132 and 0.804, respectively (including the points from 5 to 12 Å). Note that the two sets of diffuse functions in basis set 2 are not included in the three sets of diffuse functions of basis set 3; the diffuse functions of basis set 3 are entirely different functions (see the Appendix). Thus, the agreement seen in Fig. 9(b) indicates that T_{BA} is not particularly sensitive to the basis set choice, given that enough diffuse functions are included to describe the wave function in the region of R of interest.

V. HETERONUCLEAR SYSTEMS

It is also possible to consider charge transfer interactions in heteronuclear diatomic systems. The expression for the transfer probability in the two-atom case for the same conditions as in Eq. (1) is given by[31,32]

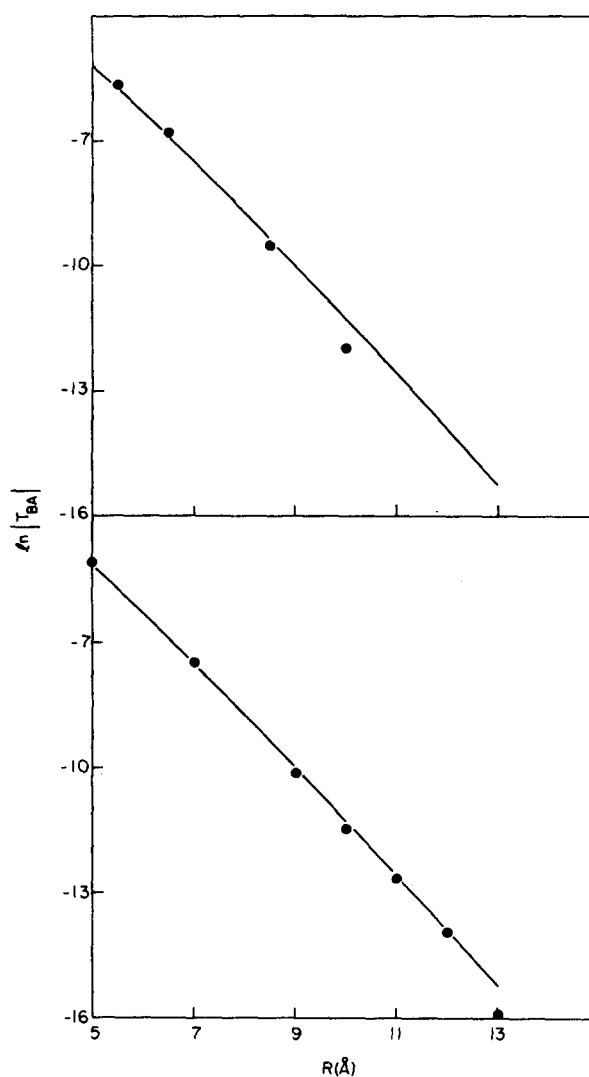$$P_{AB}(t) = A_{AB}\sin^2\left[\frac{t}{2\hbar}\sqrt{(E_A - E_B)^2 + 4T_{BA}T_{AB}}\right], \quad (14)$$

FIG. 9. Comparison of $\ln|T_{BA}|$ vs R for SCF calculations of Be_2^+ for various basis sets. In each case, the solid curve represents the fit of the three diffuse-function basis set results to the functional form $T_{BA} = A_2R^2\exp(-\alpha_2R)$. (a) The circles are results obtained for the zero diffuse function basis. (b) The circles are results obtained with the two diffuse function basis set. The parameters for the two diffuse function basis results from the fit of the form $A_2R^2\exp(-\alpha_2R)$ to the calculated points are $A_2 = 0.132$, $\alpha_2 = 0.804$.

where T_{AB} is defined analogously to T_{BA} of Eq. (4) but with H_{AA} replaced by H_{BB}, E_A, and E_B are the total energies of the initial and final states, and A_{AB} is a constant for a given set of E_A, E_B, and initial and final states (see Refs. 31 and 32). It is seen that the time dependence of the system is now controlled by two factors, an energy difference *and* $T_{BA}(T_{AB})$. We will concentrate on the second term, as it bears closest analogy to the symmetric systems examined earlier. Note, $|T_{BA}|$ and $|T_{AB}|$ will not be equal whenever $H_{AA} \neq H_{BB}$. In the results below, we present values of $(T_{BA}T_{AB})^{1/2}$ since in the limit of vanishing $E_A - E_B, (T_{BA}T_{AB})^{1/2}$ reduces to $T_{BA} = T_{AB}^*$.

In passing, it is noted that the inequality of $|T_{BA}|$ and $|T_{AB}|$ would appear to cause microscopic irreversibility

between forward and back golden rule[8,9] electron transfer rate constants from equienergetic levels in extended systems. This is, however, an artifact of the use of the Condon approximation, which assumes the insensitivity of T_{BA} to nuclear position, and thus to the difference between H_{AA} and H_{BB}. A means of circumventing this problem in solution electron-transfers is to evaluate T_{BA} at the crossing point of the reactant and product nuclear surfaces, where $H_{AA} = H_{BB}$. In a diatomic system, no such nuclear coordinates exist to equalize reactants and products electronic surfaces, and we have therefore evaluated $(T_{BA} T_{AB})^{1/2}$.

For elastic electron tunneling between two different surfaces, a golden rule analysis[23,24] suggests that electron tunneling occurs only between equienergetic levels (due to the delta function in energy in the golden rule rate expression and the continuous energy spectrum within bands of the solid), and thus $|T_{BA}|$ always equals $|T_{AB}|$ for the truly infinite system. Because of the discrete energy spectrum in a cluster, the cluster description of such transfers will not provide true equality of initial and final levels, and it is therefore necessary to consider transfers to and from a band of energy states surrounding the Fermi level.[23,24] In such cases, $|T_{BA}| \neq |T_{AB}|$ in general.

In Fig. 10(a)–10(c), plots of the quantity $\ln(T_{BA} T_{AB})^{1/2}$ as a function of R are shown for the heteronuclear systems ZnBe$^+$, ZnMg$^+$, and ZnCd$^+$. For comparison purposes, the pertinent $\ln|T_{BA}^{Zn_2^+} T_{AB}^{M_2^+}|^{1/2}$ are also shown. For ZnBe$^+$ and ZnCd$^+$, the initial and final wave functions were obtained self-consistently as localized descriptions at each R. For ZnMg$^+$, the wave functions would only localize in the form Zn–Mg$^+$, and frozen wave functions similar to those used in the symmetric systems were used in this case. Only results between 5 and 10 Å are presented for ZnMg$^+$ because of errors in the frozen wave functions similar to those encountered previously.

The values of α^{Fit} from the functional form $T_{BA} = A_2 R^2 \exp(-\alpha_2 R)$ for the cross reactions are given in Table II and can be compared with those from the symmetric systems of Table I. The values α^{Fit} are, not surprisingly, quite close to those of the symmetric cases.

Comparison of the heteronuclear $(T_{BA} T_{AB})^{1/2}$ with $(T_{BA}^{i} T_{AB}^{j})^{1/2}$, where T_{BA}^{i} and T_{AB}^{j} denote the symmetric system T_{BA} and T_{AB} corresponding to the heteronuclear ij system, shows good agreement in the case of ZnCd$^+$ but not for ZnBe$^+$, where $(T_{BA}^{i} T_{AB}^{j})^{1/2}$ is approximately 30% smaller than $(T_{BA} T_{AB})^{1/2}$.

VI. CONCLUSIONS

The present results indicate that current *ab initio* electronic structure methods utilizing Gaussian basis sets are capable of producing accurate decay rates of T_{BA} over large distances. As a result, it is reasonable to assume that such methods may be useful in examining vacuum charge transfers over large distances, as occur in applications of the scanning tunneling microscope. This accuracy reinforces the utility and reliability of the application of such techniques to shorter range transfers as are encountered, for example, in solution transition metal redox reactions.[19–21]

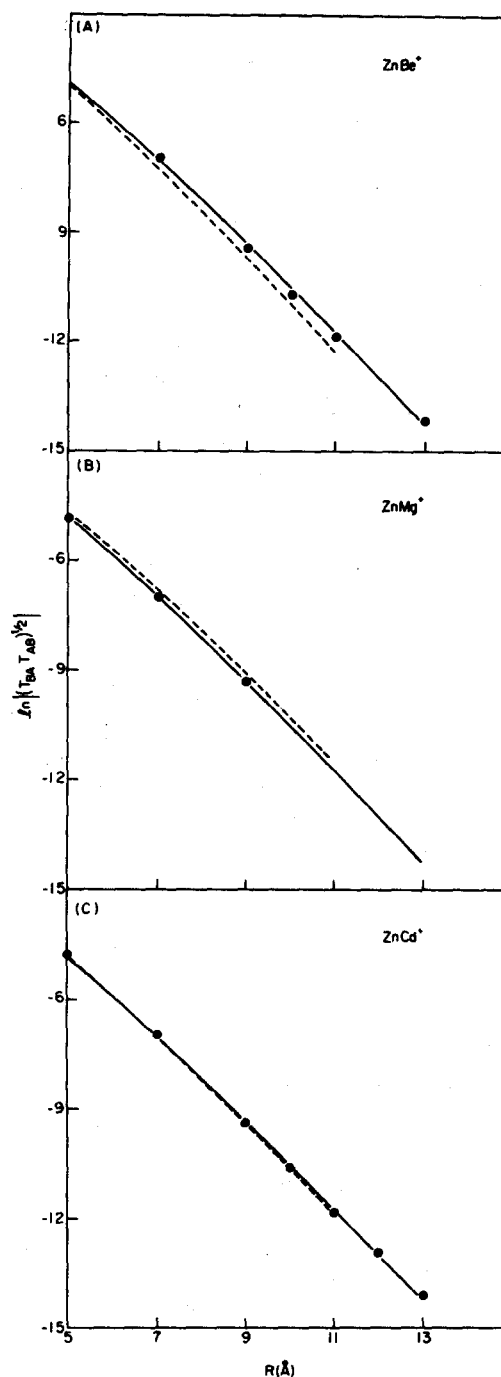Of the various methods presented here, we believe that

FIG. 10. $\ln|(T_{BA} T_{AB})^{1/2}|$ vs R for various heteronuclear diatomic systems containing Zn. In each case, the circles are the calculated data points for the Zn–M$^+$ system, the solid curve is a fit of the data to the functional form $(T_{BA} T_{AB})^{1/2} = A_2 R^2 \exp(-\alpha_2 R)$, and the dashed curve is a fit to the form $A_2 R^2 \exp(-\alpha_2 R)$ of the quantity $\ln | (T_{BA}^{Zn_2^+} T_{AB}^{M_2^+})^{1/2} |$, appropriate to the given system. (a) ZnBe$^+$ (two diffuse basis functions on Be), (b) ZnMg$^+$, (c) ZnCd$^+$.

TABLE II. Decay constants for heteronuclear diatomic systems,[a] $T_{BA} = A_2 R^2 \exp(-\alpha_2 R)$.

System	A^{Fit}	α^{Fit}
ZnBe$^+$	0.094	0.746
ZnMg$^+$	0.108	0.762
ZnCd$^+$	0.102	0.746

[a] All quantities in a.u.

the one we have termed the SCF method is the most reliable for estimating T_{BA} at large distances. Its accuracy apparently stems from the incorporation of functions on the second center in propagating the electronic interaction, while still retaining a localized description. The results obtained with these wave functions yielded exponential decays of T_{BA} with distance to better than 10 Å center-to-center separation for all systems except He.

Results for the system Be_2^+ showed that while the inclusion of diffuse functions had a qualitative effect on the value of T_{BA} at large R, the value of T_{BA} was not particularly sensitive to the choice of exponents for the diffuse basis set. The two diffuse basis sets examined had completely different s and p diffuse functions, yet yielded values of T_{BA}, and decays of T_{BA} with distance, in good agreement with each other over a wide range of distances.

It might be thought that electronic reorganization upon gain or removal of an electron could seriously alter the size of T_{BA}. However, the present results indicate that this is not a major effect. This is most easily seen in comparisons of the frozen orbital (atom + ion) and frozen orbital (atom + atom) results. In the latter case, we specifically exclude electronic reorganization upon electron transfer, yet the size of T_{BA} is similar in the two cases, as is the decay with distance. While electronic rearrangement plays some role in determining the size of T_{BA}, the role is secondary relative to orbital energy and atomic size considerations. This suggests that charge rearrangements upon ionization of metal clusters should not have a qualitative effect on the size of T_{BA}, relative to T_{BA} calculated for an infinite surface, all other effects (such as correlation, edge effects, etc.) being equal.

ACKNOWLEDGMENTS

APPPENDIX: CALCULATIONAL DETAILS

Basis sets

(a) H: The Huzinaga $7s$ basis set[33] was used contracted to four functions in the form (4,1,1,1). In addition, three diffuse Gaussian s functions were added having the exponents 0.018 22, 0.005 466, and 0.001 640.

(b) He: The Huzinaga [10s] basis set[33] for He was used, with a contraction scheme of (6,1,1,1,1). Three diffuse s Gaussians were added having orbital exponents 0.004 318, 0.001 727, and 0.000 690 9. Five uncontracted p functions were also used, having exponents 1.276, 0.2700, 0.0571,[34] 0.019 86, and 0.000 690 9.

(c) Be: For beryllium, three different basis sets were used having zero, two, and three added diffuse functions. In

each case, the Dunning–Huzinaga[35] VDZ $(9s,5p/3s,2p)$ basis set was used. For the basis set having two additional s and p sets of diffuse functions, the s Gaussians used had the exponents 0.018 76 and 0.006 029, and the p Gaussians had exponents 0.017 23 and 0.006 029. For the basis having three additional diffuse s and p functions, the s Gaussians used had the exponents 0.016 05, 0.004 413, and 0.001 213 and the p functions had the exponents 0.014 32, 0.004 168, and 0.001 213.

(d) Mg: The SHC effective potential of Rappé *et al.*[36] was used together with the DZ basis recommended there. This basis set was augmented with two sets of s and p diffuse Gaussians, the s functions having the exponents 0.016 65 and 0.006 478, and the p functions having the exponents 0.018 53 and 0.006 478.

(e) Ca: The recently developed effective potential of Wadt and Hay[26] was used to replace the Ar core. The associated $(3s, 3p)$ basis set was employed. Two additional sets of s and p Gaussians were used, the s functions having the exponents 0.009 636 and 0.002 650 and the p functions having the exponents 0.008 347 and 0.002 650.

(f) Zn: The effective potential of Hay and Wadt[27] for Zn was used, allowing for explicit treatment of the $3d^{10}$ and $4s^2$ electrons. The $(3s,2p,2d)$ basis set suggested by Hay and Wadt was augmented by two sets of additional s and p Gaussians, the s functions having the exponents 0.015 40 and 0.004 280 and the p functions having the exponents 0.012 25 and 0.004 280.

(g) Cd: The effective potential of Hay and Wadt[27] for Cd was used, allowing for explicit inclusion of the $4d^{10}$ and $5s^2$ electrons. The recommended $(3s,2p,2d)$ basis set was augmented by two sets of additional s and p Gaussians, the s functions having the exponents 0.016 32 and 0.004 896 and the p functions having the exponents 0.014 08 and 0.004 896.

Wave functions

For the calculations labeled SCF in the text, Hartree–Fock (HF) calculations were performed at each R to obtain wave functions having the character of the odd electron being localized on the right or left center, thus yielding the nominal structures M^+–M and M–M^+, respectively. No restrictions were placed on the wave functions to bring about the localization.

For the various frozen wave function calculations, HF solutions for the relevant atom and/or ion were used and combined to yield the given frozen wave function for the system. At each R, the orbitals were properly orthogonalized but otherwise were not allowed to change shape.

The frozen orbital symmetry-restricted calculation for Be_2^+ used linear combinations of Be neutral orbitals centered on each atom to construct the symmetric and antisymmetric molecular orbitals. As in the localized frozen orbital case, these orbitals were made orthogonal at each R but were otherwise not allowed to change shape.

Calculation of T_{BA}

The calculation of T_{BA} was performed using the set of programs developed by Voter and Goddard.[28] The SCF wave functions representing the left and right localized

structures [e.g., Eqs. (1) and (2)] were used in the calcula-
tion of the individual matrix elements Eqs. (5a)–(5c). Since
each oribital in the left wave function overlaps all orbitals of
the right wave function, the orbitals of the two wave func-
tions were "biorthogonalized"[28] in order to simplify the eva-
luation of the matrix elements. In the biorthogonalization
procedure, a linear transformation is applied to the orbitals
of each localized structure so that a given orbital in, for ex-
ample, the left localized wave function, will have nonzero
overlap (generally less than one) with only a single oribital
on the right localized wave function. This simplifies the ex-
pressions for the matrix elements of Eq. (5a), yielding terms
involving one- and two-electron operators between the non-
orthogonal wave functions.[28] In these calculations, an SCF
calculation leads to the localized wave functions (1) and
(2), but we do not reoptimize the orbitals *after* resonance
(the programs of Voter and Goodgame allow this, but pre-
liminary tests indicate that this much lengthier procedure
was not needed).

For Be_2^+, Zn_2^+, and Cd_2^+, the overlap of the "core"
electron (1s,3d,and 4d,respectively) on the two centers was
so small, and the change upon addition or removal of the
extra electron so slight, that explicit inclusion of the core
electrons in the calculation of T_{BA} at large distances intro-
duced significant numerical error. To correct this, these core
electrons were treated as a static field for the noncore elec-
trons for the calculation of T_{BA}, but not when obtaining the
wave functions; thus the core electronic density for T_{BA} was
the same whether the extra electron was left or right local-
ized. Since the *core* electron density is frozen in an asymme-
tric distribution, i.e, say for M–M$^+$, this could, in principle,
induce an asymmetry in $|T_{BA}|$ and $|T_{AB}|$ via differences in
H_{AA} and H_{BB}. For Be_2^+,$|T_{BA}|$ and $|T_{AB}|$ were equal to at
least three decimal places, thus substantiating this procedure
for Be_2^+. For Zn_2^+,T_{BA} was found to agree with the all-
electron $(d + s)$ calculation of T_{BA} to within 4% at the
shorter distances (5–9 Å), where the all-electron calcula-
tions could be performed. For Cd_2^+,$|T_{BA}|$ and $|T_{AB}|$ differed
by 20%–30%, but the quantity $(T_{BA}T_{AB})^{1/2}$ was found to
agree with the all-electron $(s + d)$ calculation to within 4%
over 5–8 Å, where the latter values could be obtained. Thus
it is $(T_{BA}T_{AB})^{1/2}$ that is presented in the text for the system
Cd_2^+.

[1]Cf. N. Sutin, Prog. Inorg. Chem. **30**, 441 (1983).
[2]Cf. V. G. Levich, in *Physical Chemistry: An Advanced Treatise* (Aca-
demic, New York, 1970), Vol. 9B, p. 985.
[3]Cf. D. Devault, *Quantum-Mechanical Tunneling in Biological Systems*,
2nd ed. (Cambridge University, New York 1984).
[4]R. A. Marcus and N. Sutin, Biochim. Biophys. Acta. **811**, 265 (1985).
[5]M. Baer, Ber. Bunsenges. Phys. Chem. **86**, 448 (1982).
[6](a) G. Binnig, H. Rhorer, Ch. Gerber, and E. Weibel, Appl. Phys. Lett.
40, 178 (1982); (b) Phys. Rev. Lett. **50**, 120 (1983); (c) Surf. Sci.**131**,
L379 (1983).
[7]R. A. Marcus, J. Chem. Phys. **43**, 679 (1965).
[8]V. G. Levich and R. R. Dogonadze, Collect. Czech. Chem. Commun. **26**,
193 (1961). Translator: O. Boshko, University of Ottawa, Ontario, Can-
ada.
[9]N. R. Kestner, J. Logan, and J. Jortner, J. Phys. Chem. **78**, 2148 (1974).

[10]J. J. Hopfield, Proc. Natl. Acad. Sci. USA, **71**, 3640 (1974).
[11]J. Ulstrup, *Charge Transfer Processes in Condensed Media: Lecture Notes
in Chemistry*, No. 10 (Springer, New York, 1979).
[12]P. Siders, R. J. Cave, and R. A. Marcus, J. Chem. Phys. **81**, 5613 (1984).
[13]J. V. Beitz and J. R. Miller, J. Chem. Phys. **71**, 4579 (1979).
[14]I. V. Alexandrov, R. F. Khairutdinov, and K. I. Zamaraev, Chem. Phys.
32, 123 (1978).
[15]B. Brocklehurst, J. Phys. Chem. **83**, 536 (1979).
[16]D. N. Beratan and J. J. Hopfield, J. Am. Chem. Soc. **106**, 1584 (1984).
[17]S. Larsson, J. Phys. Chem. **88**, 1321 (1981).
[18]S. Larsson, J. Am. Chem. Soc. **103**, 4034 (1984).
[19]M. D. Newton, Int. J. Quantum Chem. Symp. **14**, 363 (1980).
[20]M. D. Newton, in *Mechanistic Aspects of Inorganic Reactions*, ACS Symp.
Ser. No. 198, edited by D. B. Rorabacher and J. F. Endicott (American
Chemical Society, Washington, D. C., 1982), p. 255.
[21]J. Logan and M. D. Newton, J. Chem. Phys. **78**, 4086 (1983).
[22]N. Garcia, C. Ocal, and F. Flores, Phys. Rev. Lett. **50**, 2002 (1983).
[23]J. Tersoff and D. R. Hamann, Phys. Rev. B **31**, 805 (1985).
[24]N. D. Lang, Phys. Rev. Lett. **55**, 230 (1985).
[25]J. C. Slater, *Quantum Theory of Matter* (McGraw–Hill, New York,
1968), p. 396.
[26]W. R. Wadt and P. J. Hay, J. Chem. Phys. **82**, 284 (1985).
[27]P. J. Hay and W. R. Wadt, J. Chem. Phys. **82**, 270 (1985).
[28]A. F. Voter and W. A. Goddard III, Chem. Phys. **57**, 253 (1981).
[29]As a test of the quality of the numerical fits, we calculated

$$Y = \sum_i |\ln|T_{BA}^{calc}(R_i)| - \ln|T_{BA}^{fit}(R_i)||/n_i$$

where $T_{BA}^{calc}(R_i)$ and $T_{BA}^{fit}(R_i)$ are the values of T_{BA} obtained from the
calculated data points and the values obtained from the given fit to the
data points at the respective R_i. n_i is the number of points in the fit. For
the three diffuse function basis set for Be, we obtain $Y_0 = 0.047$,
$Y_1 = 0.059$, and $Y_2 = 0.086$, where Y_0 corresponds to Y for the fitting
function $A_0 \exp(-\alpha_0 r)$, Y_1 and Y_2 are analogously defined. For Zn we
have $Y_0 = 0.05$, $Y_1 = 0.03$, and $Y_2 = 0.04$; for Cd, $Y_0 = 0.06$, $Y_1 = 0.045$,
and $Y_2 = 0.06$; for Mg, $Y_0 = 0.13$, $Y_1 = 0.09$, and $Y_2 = 0.05$; for Ca,
$Y_0 = 0.17$, $Y_1 = 0.10$, $Y_2 = 0.10$. The fits are good in all cases, the values
of Y_1 are usually somewhat lower, but the values of α_2 are consistently in
better agreement with $\alpha^{Koopmans}$.
[30]C. C. J. Roothan, J. Chem. Phys. **19**, 1445 (1951).
[31]R. P. Feynman, R. B. Leighton, and M. Sands, *The Feynman Lectures on
Physics*, 2nd ed. (Addison–Wesley, Reading, 1965), Chap. 9.
[32]In the derivation of Eq. (14), an analysis entirely analogous to that of Ref.
31 was used, with two exceptions. First, while a two-state model is as-
sumed here, the nonzero overlap of the two "states" was explicitly treated.
Second, since the two states overlap, we used the modified projection op-
erators

$$P_A' = \frac{|A\rangle(\langle A| - S_{AB}\langle B|)}{1 - |S_{AB}|^2}$$

and

$$P_B' = \frac{|B\rangle(\langle B| - S_{BA}\langle A|)}{1 - |S_{BA}|^2},$$

rather than the conventional $P_A = |A\rangle\langle A|$ and $P_B = |B\rangle\langle B|$ in obtain-
ing the final expression for $P_{AB}(t)$. Operation with P_A' or P_B' on
$\Psi(t) = C_A(t)|A\rangle + C_B(t)|B\rangle$ yields $C_A(t)|A\rangle$ or $C_B(t)|B\rangle$ respec-
tively. This simplifies the expression for $P_{AB}(t)$, but also slightly modifies
its definition. Use of conventional projection operators leads to the defini-
tion of $P_{AB}(t)$ as the probability of the system being in state A at time t.
Use of P_A' or P_B' leads to $P_{AB}(t)$ as the probability of $C_A(t)$ being nonzero
at time t when its initial value was zero at $t = 0$. For the purpose of illus-
trating the behavior of $(T_{BA}T_{AB})^{1/2}$ in the mixed systems, the distinction
is not important.
[33]S. Huzinaga, J. Chem. Phys. **42**, 1293 (1965).
[34]The three largest He p exponents were obtained by M. J. Brusich and W.
A. Goddard III (unpublished results).
[35]T. H. Dunning Jr. and P. J. Hay, in *Methods of Electronic Structure The-
ory*, edited by H. F. Schaefer III (Plenum, New York, 1977), p. 1.
[36]A. K. Rappé, T. A. Smedley, and W. A. Goddard III, J. Phys. Chem. **85**,
1663 (1981).